PROCEEDINGS OF SCIENCE

Measurements of collective behavior in pp, Xe+Xe, and Pb+Pb collisions with the ATLAS detector

Somadutta Bhatta (On behalf of the ATLAS Collaboration)[a,*]

[a] *Stony Brook University,*
Sttony Brook, New York, USA-11790

E-mail: somadutta.bhatta@stonybrook.edu

Results from two measurements on the collective flow phenomena in a variety of collision systems using the ATLAS detector at the Large Hadron Collider (LHC) are presented. First, the measurement of the sensitivity of two-particle correlations in pp collisions at 13 TeV to the presence of jets is presented. Rejecting particles associated with low-p_{T} jets can help verify the role of semi-hard processes in the collective behaviour observed in pp collisions. Second, a new measurement on the correlation between the event-wise average transverse momentum ($[p_{\mathrm{T}}]$) and the harmonic flow (v_n) for Pb+Pb collisions at 5.02 TeV and Xe+Xe collisions at 5.44 TeV is demonstrated for harmonics $n = 2$, 3, and 4. This correlation quantified by measurement of the Pearson correlator between v_n and $[p_{\mathrm{T}}]$ carries important information about the initial-state geometry of the Quark-Gluon Plasma. Additionally, the potential quadrupole deformation in Xe+Xe is predicted to produce an initial state with enhanced shape and size fluctuations, and result in non-trivial change in the correlation.

**** The European Physical Society Conference on High Energy Physics (EPS-HEP2021), ****
**** 26-30 July 2021 ****
**** Online conference, jointly organized by Universität Hamburg and the research center DESY ****

*Speaker

ATL-PHYS-PROC-2021-066
29 September 2021

PoS(EPS-HEP2021)305

1. Introduction and Measurements

Heavy-ion collisions at the Large Hadron Collider produce Quark-Gluon Plasma (QGP) whose space-time evolution is well described by relativistic viscous hydrodynamics [1]. Driven by the large pressure gradients, the QGP expands rapidly in the transverse plane, which converts the spatial anisotropy in the initial state into momentum anisotropy in the final momentum space. The collective expansion in each event is quantified by a Fourier expansion of particle distribution in azimuth given by

$$\frac{\mathrm{d}N}{\mathrm{d}\phi} \propto \left(1 + 2\sum_{n=1}^{\infty} v_n \cos\left(n\left(\phi - \Phi_n\right)\right)\right) \tag{1}$$

where the v_n and Φ_n denote the magnitude and orientation of the single-particle anisotropies respectively. The two-particle correlations (2PC) in relative azimuthal angle $\Delta\phi$ and with pseudorapidity separation $\Delta\eta$ show distinct long-range correlations along $\Delta\eta$ [2] arising from a convolution of the single-particle anisotropies v_n. The long-range correlations were not expected to be seen in smaller colliding systems (proton-nucleus (p+A) or proton-proton (pp)). Investigations of the long-range correlations in pp collisions by the ATLAS Collaboration attributed the long-range correlations to single-particle anisotropies similar to those in heavy-ion collisions [3]. However, it has been argued that the ridge may arise from hard or semi-hard processes as well. In these processes multi-particle correlations between outgoing partons may arise due to saturation of the parton configurations in the incident hadrons [4]. A study of hard-scattering processes at parton (jet) transverse momentum scales $p_{\mathrm{T}} > 10$ GeV may provide new insight into the origin of the ridge in pp collisions. If the long-range correlations arise due to hard or semi-hard processes, then removing particles associated with jets from the analysis would weaken the long-range correlation.

The analysis ([5] and references therein) uses jets reconstructed from tracks ("track-jets") using the ATLAS detector [6]. The jet reconstruction procedure uses the anti-$\mathrm{k_T}$ algorithm with a radius parameter of R = 0.4. The transverse momentum of the jets and the number of constituents are corrected to account for the average combinatorial contribution of underlying event (UE) tracks. Additionally, for the template-fits, the peripheral reference $C^{\mathrm{periph}}(\Delta\phi)$ is constructed using events with (efficiency corrected) multiplicity ($\mathrm{N_{ch}^{rec,corr}}$) < 20. Tracks within $\Delta\eta = \pm 1$ from the jet axis of any jets with $\mathrm{p_{T,jet}} > 10$ GeV are dropped from the 2PC analysis. This rejection procedure [7] removes slices of the detector acceptance for all ϕ values.

The events are categorized into four classes for which the v_n measurements are performed: **Inclusive**: Analysis with no rejection of tracks based on a presence of jet. **AllEvents**: Analysis with tracks within one unit in η from any jet above the chosen threshold (10 GeV) removed from the 2PC analysis. **NoJet**: Analysis performed using events that do not have even a single jet with p_{T} greater than the chosen threshold. This sample is composed of events dominated by soft processes. **WithJet**: Analysis performed on events that have at least one jet with p_{T} greater than the chosen p_{T} threshold. The tracks within one unit in η of any such jets are removed from the 2PC analysis. NoJet and WithJet samples add up to the AllEvents sample.

A comparison of multiplicity dependence of the v_n for n = 2-3 from the AllEvents and NoJet to the Inclusive pp results (Figure 1) shows that v_n values vary weakly with multiplicity. It is observed that the v_2 values in the AllEvents and NoJet samples, where tracks associated with jets are removed or not present, are only marginally smaller (within 2–5%) than in the Inclusive sample where no

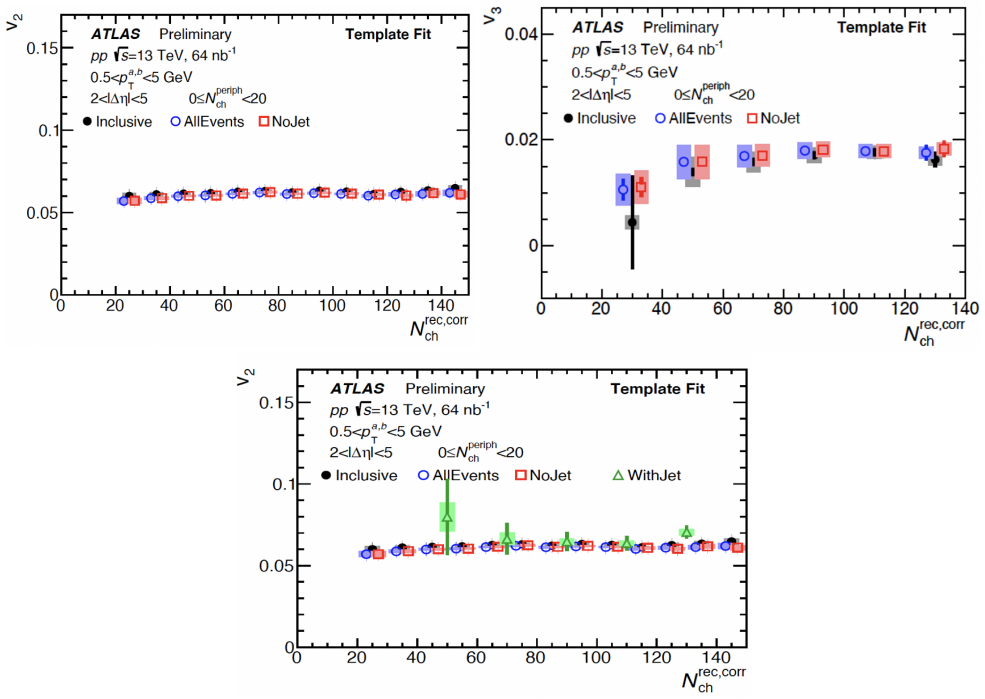

Figure 1: (Top) The v_2 and v_3 as a function of the (efficiency corrected) multiplicity. The data-points for the Inclusive sample are drawn at the nominal values, AllEvents and NoJet points are shifted slightly for clarity. The error bars and shaded bands correspond to statistical and systematic uncertainties respectively. (Bottom) v_2 as a function of the (efficiency corrected) multiplicity including WithJet sample results [5].

jet rejections are applied. This difference can partially arise from the softening of the p_{T}-spectra when removing tracks associated with jets, which affects the p_T integrated v_2 over the 0.5–5 GeV p_{T} range. Another contribution to the change in the v_2 can be due to residual changes in the shape of the dijet correlations, that are not accounted for in the template fits, which are mitigated when explicitly rejecting jets as in the AllEvents and NoJet samples. The results for the v_2 in the WithJet sample are consistent with the v_2 in the Inclusive sample within uncertainties. For the harmonic v_3, the trend of the change is opposite to that for v_2 for the AllEvents and NoJet samples, where the v_3 values are larger compared to the Inclusive sample. The correlations arising from dijets typically affect the even and odd-harmonics oppositely. The relative effect of such biases on the v_3 can be larger, as the magnitude of the v_3 is much smaller than that of the v_2. The results for the WithJet sample are statistically significant only for the v_2 and are not shown for the v_3 measurements.

The n^{th}-order azimuthal flow vector is driven by the hydrodynamic response and is proportional to the initial spatial anisotropy characterized by eccentricity vectors $\mathcal{E}_n = \epsilon_n e^{\mathrm{i}n\Psi_n}$. In addition to generating anisotropic flow, the hydrodynamic response to the overall transverse size ($\mathrm{R_T}$) also leads to large "radial flow", reflected by an increase of the $[p_{\mathrm{T}}]$. In particular, events with similar total energy, but smaller $\mathrm{R_T}$ in the initial state are expected to have stronger radial expansion and therefore larger $[p_{\mathrm{T}}]$ [8]. Therefore the event-by-event (EbE) fluctuation of the $\mathrm{R_T}$ would also lead to EbE fluctuation of $[p_{\mathrm{T}}]$, characterized by its variance $c_k = \langle \delta p_{\mathrm{T}} \delta p_{\mathrm{T}} \rangle$, $\delta p_{\mathrm{T}} = p_{\mathrm{T}} - [p_{\mathrm{T}}]$. Furthermore, any correlated fluctuations between the $\mathcal{E}_n$ and R in the initial state is expected to

generate dynamical correlation between $\boldsymbol{V}_n$ and $[p_{\mathrm{T}}]$ in the final state. A three-particle correlator has been proposed to quantify this correlation:

$$\rho(v_n^2, [p_{\mathrm{T}}]) = \frac{\left\langle v_n^2, p_{\mathrm{T}} - [p_{\mathrm{T}}] \right\rangle}{\sqrt{\left\langle v_n^4 \right\rangle - \left\langle v_n^2 \right\rangle^2}\sqrt{c_k}} \left(\equiv \frac{\mathrm{cov_n}}{\sqrt{\mathrm{var_n}}\sqrt{c_k}} \right) \tag{2}$$

where the averages are over events with similar particle multiplicity. An investigation on the system-size dependence of $v_n - [p_{\mathrm{T}}]$ correlation is performed in ^{129}Xe+^{129}Xe collisions and comparing them with ^{208}Pb+^{208}Pb collisions ([9] and references therein) . Recent measurements show that the v_n exhibits significant differences between these two systems, especially in the central collisions where the difference is much larger. Model calculations show that these differences are compatible with the expected ordering of the eccentricities and roles of viscous effects in the two systems. In particular, the large difference in central collisions is related to the non-negligible deformation present in the ^{129}Xe nuclei; such deformation effects were recently predicted to have a even stronger effect for $v_n - [p_{\mathrm{T}}]$ correlation. In addition to these initial-state driven long-range global correlations, the $v_n - [p_{\mathrm{T}}]$ correlation measurement may have short-range "non-flow" correlations from resonance decays and jets. The non-flow correlation is suppressed and quantified by requiring correlation between particles from different subevents separated in η (two subevent method (2SE), three subevent method (3SE)) [10].

The measurement of the $\mathrm{cov_n}$, $\mathrm{var_n}$ and c_k follows similar procedure as detailed in Ref. [11]. In the first step, these correlators are first calculated in each event as average over all combinations from particles from a given η and p_{T} range. Next, the value obtained in each event are averaged over events with similar multiplicity, defined as events with similar FCal-$\mathrm{E_T}$ (matched within 0.002 TeV) or those with same number of reconstructed charged particles within $0.5 < p_{\mathrm{T}} < 5$ GeV and $|\eta| < 2.5$ ($N_{\mathrm{ch}}^{\mathrm{rec}}$). They are then combined in broader multiplicity ranges of the event ensemble to obtain statistically more precise results. Effects of centrality fluctuations between different event classes are discussed by comparing the results obtained from FCal-$\mathrm{E_T}$ and $N_{\mathrm{ch}}^{\mathrm{rec}}$.

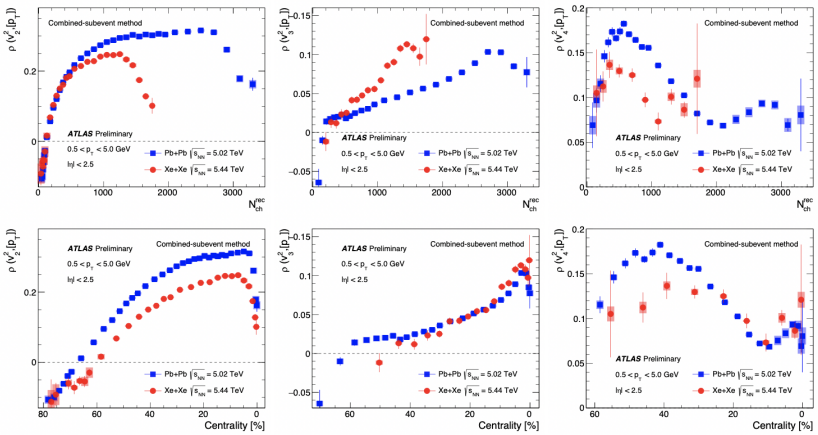

Figure 2: Comparison of $\rho(v_n\{2\}^2, [p_{\mathrm{T}}])$ between Xe+Xe and Pb+Pb for n =2, 3 and 4 plotted as a function of $N_{\mathrm{ch}}^{\mathrm{rec}}$ (top), FCal-ΣE_{T} based centrality (bottom) in $0.5 < p_{\mathrm{T}} < 5$ GeV. The error bars and shaded area represent statistical and systematic uncertainties respectively [9].

The $\rho(v_n^2, [p_T])$ as a function of N_{ch}^{rec}, is smaller in Xe+Xe than in Pb+Pb for $n = 2$ and 4, but larger in Xe+Xe than in Pb+Pb for $n = 3$. The trends are different for centrality dependence where the signal is smaller in Xe+Xe than Pb+Pb for $n = 2$ but comparable for $n = 3$ and 4. The magnitude of $\rho(v_2^2, [p_T])$ is much smaller in Xe+Xe than Pb+Pb and could have contributions from deformation in Xe nuclei. Figure 3 shows the comparison of $\rho(v^2_{(n=2,3)}, [p_T])$ in Xe+Xe and Pb+Pb collisions from CGC-Hydro as a function of N_{ch}^{rec}-based centrality and ΣE_T-based centrality. The CGC-Hydro model does not capture the qualitative trends between Xe+Xe and Pb+Pb and shows comparable magnitude for the two systems. The model calculations have large uncertainties and do not explain the measurement qualitatively or quantitatively.

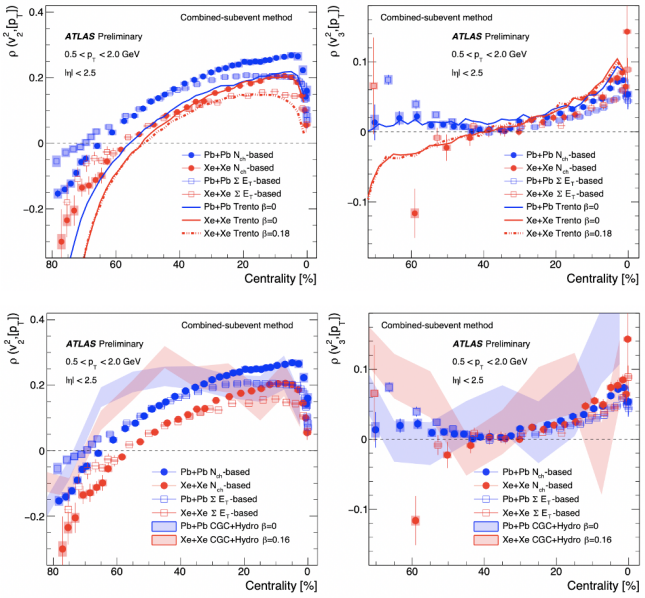

Figure 3: Comparison of $\rho(v_n\{2\}^2, [p_T])$ in Xe+Xe and Pb+Pb with Trento model for n=2 and 3 as a function of N_{ch}^{rec}-based centrality and as a function of ΣE_T-based centrality in 0.5-2 GeV range (top). Similar comparison with hydro model shown in bottom panels. Error bars and shaded area represent statistical and systematic uncertainties respectively [9].

2. Summary

The measurement of two-particle correlations by rejecting particles associated with low-p_T jets indicate that the long-range correlations seen in pp collisions are only slightly affected when particles associated with hard or semi-hard processes in the event are removed. Therefore, the contribution of semi-hard processes to the ridge in pp collisions is negligible. The Pearson correlator $\rho(v_n^2, [p_T])$ shows similar N_{ch}^{rec}-dependent trends between the two collisions systems whereas as a function of centrality, an approximate scaling behavior for $n = 3$ and 4 is observed, but $\rho(v_2^2, [p_T])$ is lower in Xe+Xe than Pb+Pb. Centrality fluctuations is observed to play an important role in these observables. Hydrodynamic and initial state models can only match the data qualitatively but fail to describe the data quantitatively. Further improvements of these models are required in order to reproduce the data obtained using the ATLAS detector at the LHC and extract

information about the initial state and transport properties of the QGP medium created in these collisions.

References

[1] Charles Gale, Sangyong Jeon, and Bjoern Schenke. "Hydrodynamic Modeling of Heavy-Ion Collisions". *Int. J. Mod. Phys. A* 28 (2013), p. 1340011. DOI: 10.1142/S0217751X13400113. arXiv: 1301.5893 [nucl-th].

[2] ALICE Collaboration. "Harmonic decomposition of two-particle angular correlations in Pb-Pb collisions at $\sqrt{s_{NN}}$ = 2.76 TeV". *Phys. Lett. B* 708 (2012), pp. 249–264. DOI: 10.1016/j.physletb.2012.01.060. arXiv: 1109.2501 [nucl-ex].

[3] ATLAS Collaboration. "Observation of Long-Range Elliptic Azimuthal Anisotropies in $\sqrt{s}$ =13 and 2.76 TeV pp Collisions with the ATLAS Detector". *Phys. Rev. Lett.* 116.17 (2016), p. 172301. DOI: 10.1103/PhysRevLett.116.172301. arXiv: 1509.04776 [hep-ex].

[4] Adrian Dumitru et al. "The Ridge in proton-proton collisions at the LHC". *Phys. Lett. B* 697 (2011), pp. 21–25. DOI: 10.1016/j.physletb.2011.01.024. arXiv: 1009.5295 [hep-ph].

[5] "Measurement of the sensitivity of two particle correlations in pp collisions at $\sqrt{s}$ = 13 TeV to the presence of jets with the ATLAS detector (ATLAS-CONF-2020-018)" (June 2020). URL: https://cds.cern.ch/record/2720248.

[6] ATLAS Collaboration. "The ATLAS Experiment at the CERN Large Hadron Collider". *JINST* 3 (2008), S08003. DOI: 10.1088/1748-0221/3/08/S08003.

[7] ATLAS Collaboration. "Transverse momentum and process dependent azimuthal anisotropies in $\sqrt{s_{\mathrm{NN}}}$ = 8.16 TeV p+Pb collisions with the ATLAS detector". *Eur. Phys. J. C* 80.1 (2020), p. 73. DOI: 10.1140/epjc/s10052-020-7624-4. arXiv: 1910.13978 [nucl-ex].

[8] Piotr Bozek and Wojciech Broniowski. "Transverse-momentum fluctuations in relativistic heavy-ion collisions from event-by-event viscous hydrodynamics". *Phys. Rev. C* 85 (2012), p. 044910. DOI: 10.1103/PhysRevC.85.044910. arXiv: 1203.1810 [nucl-th].

[9] ATLAS Collaboration. "Measurement of flow and transverse momentum correlations in Pb+Pb collisions at $\sqrt{s_{\mathrm{NN}}}$ = 5.02 TeV and Xe+Xe collisions at $\sqrt{s_{\mathrm{NN}}}$ = 5.44 TeV with the ATLAS detector (ATLAS-CONF-2021-001)" (Jan. 2021). URL: https://cds.cern.ch/record/2748818.

[10] Jiangyong Jia, Mingliang Zhou, and Adam Trzupek. "Revealing long-range multiparticle collectivity in small collision systems via subevent cumulants". *Phys. Rev. C* 96.3 (2017), p. 034906. DOI: 10.1103/PhysRevC.96.034906. arXiv: 1701.03830 [nucl-th].

[11] ATLAS Collaboration. "Measurement of long-range multiparticle azimuthal correlations with the subevent cumulant method in pp and $p + Pb$ collisions with the ATLAS detector at the CERN Large Hadron Collider". *Phys. Rev. C* 97.2 (2018), p. 024904. DOI: 10.1103/PhysRevC.97.024904. arXiv: 1708.03559 [hep-ex].